J Pharmacol Sci **112**, 64 – 72 (2010)

Journal of Pharmacological Sciences
©2010 The Japanese Pharmacological Society

Full Paper

The Guanylyl Cyclase Activator YC-1 Directly Inhibits the Voltage-Dependent K^+ Channels in Rabbit Coronary Arterial Smooth Muscle Cells

Won Sun Park[1,†], Jae-Hong Ko[2,†], Eun A Ko[1], Youn Kyoung Son[3], Da Hye Hong[1], In Duk Jung[4], Yeong-Min Park[4], Tae-Hoon Choi[5], Nari Kim[1], and Jin Han[1,*]

[1]*National Research Laboratory for Mitochondrial Signaling, Department of Physiology, College of Medicine, Cardiovascular and Metabolic Disease Center, FIRST Mitochondrial Research Group, Biomarker Medical Research Center, Inje University, Busan, 613-735 Korea*
[2]*Department of Physiology, College of Medicine, Chung-Ang University, Seoul, 156-756 Korea*
[3]*Université Paris-Sud 11, Faculté de Pharmacie, Châtenay-Malabry, 92290 France*
[4]*Department of Microbiology and Immunology and National Research Laboratory of Dendritic Cell Differentiation & Regulation, Medical Research Institute, Pusan National University, College of Medicine, Pusan, 626-770 Korea*
[5]*Department of Physical Education, Andong Science College, Andong, 760-709 Korea*

Received August 12, 2009; Accepted November 6, 2009

Abstract. We investigated the effects of YC-1, an activator of soluble guanylyl cyclase (sGC), on voltage-dependent K^+ (Kv) channels in smooth muscle cells from freshly isolated rabbit coronary arteries by using the whole-cell patch clamp technique. YC-1 inhibited the Kv current in a dose-dependent fashion with an apparent K_d of 9.67 μM. It accelerated the decay rate of Kv channel inactivation without altering the kinetics of current activation. The rate constants of association and dissociation for YC-1 were 0.36 ± 0.01 $\mu M^{-1} \cdot s^{-1}$ and 3.44 ± 0.22 s^{-1}, respectively. YC-1 did not have a significant effect on the steady-state activation and inactivation curves. The recovery time constant from inactivation was decreased in the presence of YC-1, and application of train pulses (1 or 2 Hz) caused a progressive increase in the YC-1 blockade, indicating that YC-1–induced inhibition of Kv currents is use-dependent. Pretreatment with Bay 41-2272 (also a sGC activator), ODQ (a sGC inhibitor), or Rp-8-Br-PET-cGMPs (a protein kinase G inhibitor) did not affect the basal Kv current and also did not significantly alter the inhibitory effect of YC-1. From these results, we suggest that YC-1 directly inhibits the Kv current independently of sGC activation and in a state-, time-, and use-dependent fashion.

Keywords: YC-1, voltage-dependent K^+ channel, guanylyl cyclase, coronary artery

Introduction

Guanylyl cyclases catalyze the conversion of guanosine triphosphate (GTP) to guanosine 3′5′-cyclic monophosphate (cyclic GMP), which has been regarded as an important signaling molecule in various cells and tissues. Guanylyl cyclases occur in both membrane-bound and soluble forms (1). While the membrane-bound guanylyl cyclase is activated by extracellular agonists, soluble guanylyl cyclase (sGC) contains a prosthetic heme group and acts as an important intracellular receptor for nitric oxide (NO) (2). In vascular smooth muscle, sGC is the predominant intracellular NO receptor, and the physiological actions of NO occur via the activation of sGC (3).

YC-1, a cell-permeable derivative of benzylindazole, is a potent activator of sGC in various cells (4). It increases the activity of purified sGC by approximately 10 times, independent of NO (5, 6). In the vascular system, YC-1–induced activation of sGC increases levels of cGMP, which subsequently induces vascular relaxation

†These authors contributed equally to this work.
*Corresponding author. phyhanj@inje.ac.kr
Published online in J-STAGE
doi: 10.1254/jphs.09228FP

by activating the Ca^{2+}-activated K^+ (BK_{Ca}) channel (5, 7, 8). Therefore, YC-1 is a very useful tool for studying the guanylyl cyclase / cGMP signaling pathway in vascular systems, but its undesired effects on other targets limit its usefulness in native cell systems.

Voltage-dependent K^+ (Kv) channels expressed in vascular smooth muscle participate in regulating membrane potential (9, 10). Inhibition of the Kv channels by 4-aminopyridine causes the depolarization and vasoconstriction in various arteries (11, 12). Given the usefulness of YC-1 and the physiological importance of Kv channels in the vascular system, a thorough understanding of all of the actions of YC-1 on Kv channels is essential for the accurate interpretation of experimental results obtained using this substance. Therefore, in the present study, we investigated the effect of YC-1 on Kv channels in freshly isolated coronary arterial smooth muscle cells. Our major finding was that YC-1 directly inhibits Kv channels in a state-, time-, and use-dependent fashion, that is completely independent of sGC activity.

Materials and Methods

Cell isolation

New Zealand White rabbits (2.1 – 2.4 kg) of either sex were anaesthetized with sodium pentobarbitone (50 mg/kg) and were injected simultaneously with heparin (100 U/kg) into the ear vein. The left descending coronary arteries were isolated and cleaned of the adventitia and endothelium in the normal Tyrode solution. The arteries were transferred to Ca^{2+}-free normal Tyrode solution for 20 min and then incubated in the Ca^{2+}-free normal Tyrode solution containing papain (1 mg/ml), dithiothreitol (DTT, 1.5 mg/ml), and bovine serum albumin (BSA, 1.5 mg/ml) for 25 min. The arteries were further incubated in the Ca^{2+}-free solution containing collagenase (2.8 mg/ml, 191 units/mg; Wako, Osaka), 1.5 mg/ml DTT, and 1.5 mg/ml BSA for 20 min. Single smooth muscle cells were obtained by gentle agitation with a Pasteur pipette in Kraft-Brühe (KB) solution, stored in the refrigerator, and used on the day of preparation.

Solutions and chemicals

The normal Tyrode solution contained 143 mM NaCl, 5.4 mM KCl, 0.33 mM NaH_2PO_4, 0.5 mM $MgCl_2$, 1.8 mM $CaCl_2$, 5.0 mM HEPES, and 16.6 mM glucose, adjusted with NaOH to pH 7.4. The KB solution contained 70 mM KOH, 50 mM L-glutamate, 55 mM KCl, 20 mM taurine, 20 mM KH_2PO_4, 3 mM $MgCl_2$, 0.5 mM EGTA, 10 mM HEPES, and 16.6 mM glucose, adjusted with KOH to pH 7.3. The pipette solution contained 105 mM K-aspartate, 25 mM KCl, 5 mM NaCl, 1 mM $MgCl_2$, 4 mM Mg-ATP, 10 mM BAPTA, and 10 mM HEPES, adjusted with KOH to pH 7.25. To minimize the activity of K_{ATP} and Ca^{2+}-activated currents, we included 4 mM Mg-ATP and 10 mM BAPTA in the pipette solution. In all experiments, the bath solution contained iberiotoxin (100 nM) to block the BK_{Ca} channel. All pharmacological compounds were dissolved in distilled water or in dimethyl sulfoxide (DMSO) to make stock solutions, which were diluted in the normal Tyrode solution to the concentration used. The concentration of DMSO in the final solution was less than 0.1%, and we confirmed that this concentration of DMSO did not affect the currents that were recorded. YC-1, Bay 41-2272, 1*H*-[1,2,4]oxadiazolol-[4,3-*a*]quinoxalin-1-one (ODQ), and iberiotoxin was purchased from Sigma Chemical Co (St. Louis, MO, USA). Rp-8-Br-PET-cGMPs were purchased from Biolog Life Science Institute (Bremen, Germany).

Electrophysiology and data analyses

The whole cell currents were recorded from single smooth muscle cells using patch clamp technique. An Axonpatch-1C amplifier (Axon instruments, Union, CA, USA) and digital interface (NI-DAQ 7; National Instruments, Union, CA, USA) coupled to an IBM-compatible computer were used for patch clamp and data acquisitions. All experimental parameters were controlled using Patchpro software developed by our group. The patch pipettes were made from thin-walled borosilicate glass (Clark Electromedical Instruments, Pangbourne, UK) using a puller (pp-83; Narishige, Tokyo). We used patch pipettes with a resistance of 2 – 3 MΩ, when filled with the pipette solutions.

Origin 6.0 software (Microcal Software, Inc., Northampton, MA, USA) was used for data analysis as described previously (13, 14). A first-order blocking scheme was used to describe drug-channel interaction kinetics (15). From this concept, the apparent affinity constant (K_d) and Hill coefficient (n) were obtained by fitting concentration-dependence data to the following Hill equation:

$$f = 1 / \{1 + (K_d / [D])^n\}$$

, where f means the fractional block ($f = 1 - I_{drug} / I_{control}$) at various drug concentrations [D].

The activation kinetics was calculated by fitting with a single exponential function, which was considered to be the dominant time constant of activation (13, 16). The time courses of the current during inactivation were fitted to a single (control) or double exponential function (presence of YC-1). The apparent rate constants for binding (k_{+1}) and unbinding (k_{-1}) were obtained from the following equation:

$$1 / \tau_D = k_{+1}[D] + k_{-1}$$

$$K_d = k_{-1} / k_{+1}$$

, where τ_D is the time constant of drug-induced block.

The experimental points were calculated as follows:

Normalized $I = (I - I_c) / (I_{max} - I_c)$

, where I_{max} is the maximal current measured at the most hyperpolarized preconditioning pulse and I_c is a nonzero current that was not inactivated. We subtracted this non-zero residual current from the actual values.

Activation curves were fitted with a Boltzmann distribution:

$y = 1 / \{1 + \exp(-(V - V_{1/2}) / k)\}$

, where k = slope factor, V = test potential, and $V_{1/2}$ = voltage of half-maximal conductance. The steady-state inactivation data were studied by using a two-pulse protocol; currents were measured with a 300-ms-long test potential to +40 mV, and 8-s preconditioning pulses were varied from −80 to +30 mV stepped by 10 mV in the absence and presence of drugs. The resulting steady-state inactivation data were fitted with another Boltzmann equation:

$y = 1 / \{1 + \exp((V - V_{1/2}) / k)\}$

, where V = preconditioning potential, $V_{1/2}$ = potential of the half-inactivation point, and k = slope value.

Results are expressed as means ± S.E.M. Student's t-test was used for the test of significance ($P < 0.05$).

Results

YC-1–induced inhibition of the Kv current in rabbit coronary arterial smooth muscle cells

We used whole-cell patch-clamp techniques to investigate the effect of YC-1 on Kv channels in smooth muscle cells from rabbit coronary arteries. Under control conditions, the Kv current was rapidly activated to its peak and then slowly and partially inactivated during depolarization above +20 mV (Fig. 1A), as reported previously (10, 14). Decaying outward tail currents were recorded upon repolarization to −40 mV. As shown in Fig. 1, exposure to 10 μM YC-1 inhibited the Kv current throughout the entire voltage range of activation. Inhibition occurred within 2 min of switching to YC-1–containing solution. Analysis of the peak and steady-state of the current-voltage (*I-V*) relationship for the Kv current in the absence and presence of YC-1 showed that YC-1 predominantly affected the steady-state Kv current rather than the peak current (Fig. 1: B and C). Washout partially reversed YC-1–induced inhibition (<50%, data not shown).

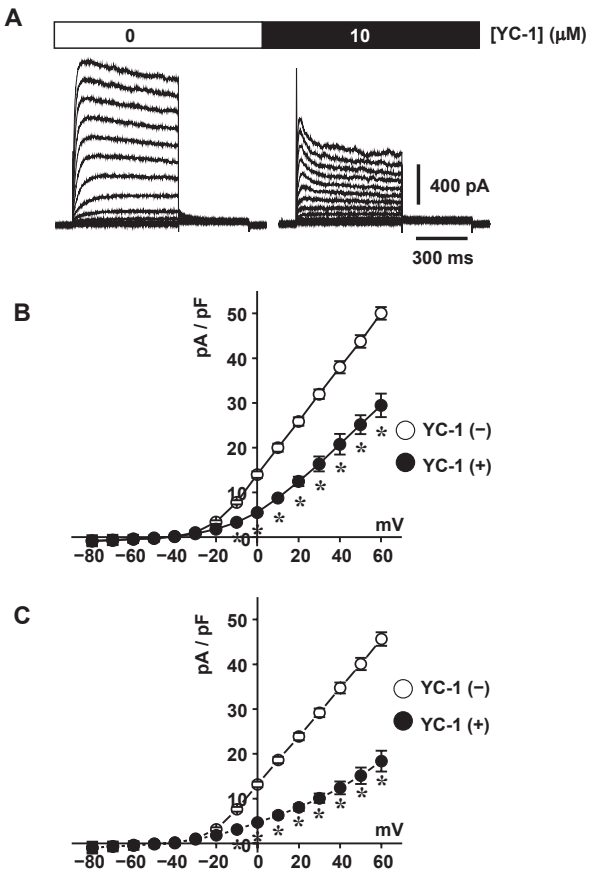

Fig. 1. Effects of YC-1 on the voltage-dependent K^+ (Kv) current in rabbit coronary arterial smooth muscle cells. A: Superimposed current traces are shown for 600-ms depolarizing pulses between −80 and +60 mV from a holding potential of −80 mV in steps of 10 mV under the control and in presence of 10 μM YC-1, respectively. B: Current-voltage (*I-V*) relationships of the peak Kv currents in the absence (open circle) and presence (closed circle) of 10 μM YC-1 (n = 6). C: *I-V* relationship of the steady-state Kv current in the absence (open circle) and presence (closed circle) of YC-1 (n = 6). The peak Kv current was measured within 80 ms of the pulse, and the steady-state Kv current was measured at the end of the pulses. *$P < 0.05$, compared to the control.

Concentration dependence of inhibition of Kv currents by YC-1

The concentration dependence of Kv channel inhibition by YC-1 is shown in Fig. 2. Representative traces of the Kv current in the presence of 3, 10, and 30 μM YC-1 are shown in Fig. 2A. As illustrated in Fig. 1, YC-1–induced inhibition of the Kv current was greater for the steady-state current than for the peak current. For the steady-state inhibition, a non-linear least-squares fit of the concentration–response equation (Hill equation) to the individual data points yielded an apparent K_d of 9.67 ± 1.23 μM and a Hill coefficient of 1.06 ± 0.12.

Concentration dependence of the time course of Kv channel inhibition

We next examined the time course of Kv channel inhibition by YC-1. The activation process data were fit to a single exponential function. Under control conditions, the time constant for activation of the Kv current was 7.96 ± 0.44 ms (n = 5), elicited by 600-ms depolarizing pulses from a holding potential of −60 mV to +60 mV.

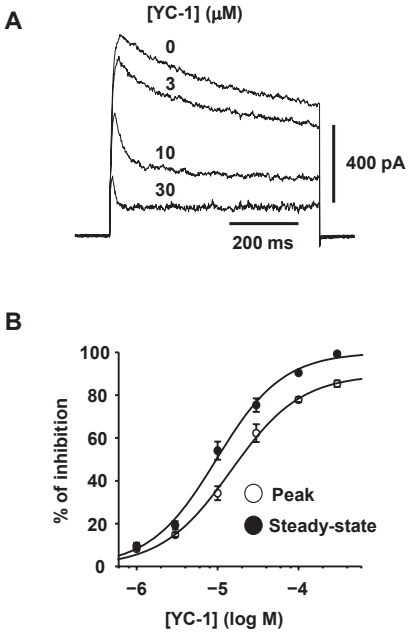

Fig. 2. Concentration dependence of YC-1–induced blocking of the Kv current. A: Current traces obtained in the absence (Control) and presence of 3, 10, and 30 μM YC-1. Whole-cell Kv currents were elicited by 600-ms depolarization to +60 mV from a holding potential of −60 mV. B: Concentration–response curve for YC-1–induced inhibition of the Kv current was measured at peak (open circle) and at steady-state (closed circle) and normalized to the current observed in the absence of each drug. The normalized currents were fit to the Hill equation (all n = 7).

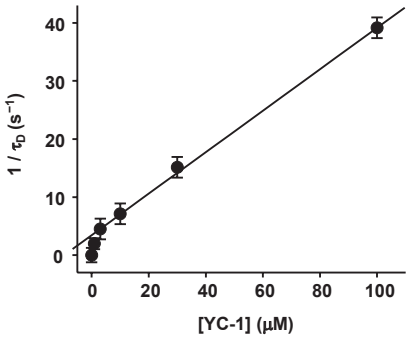

Fig. 3. Time constant of the YC-1 blockade as a function of YC-1 concentration. Apparent current decay time constants (τ_D) were obtained using single (control) and double (in the presence of YC-1) exponential fits to the falling phases of the tracings shown in Fig. 2A. The reciprocal of the drug-induced time constant obtained at +40 mV was plotted against the various concentrations (n = 5). The solid line represents a least-squares fit of the data to the relation $1 / \tau_D = k_{+1}[D] + k_{-1}$. Association ($k_{+1}$) and dissociation ($k_{-1}$) time constants were calculated using the slope and intercept value of the fitted line.

In the presence of 10 μM YC-1, the time constant was 7.91 ± 0.37 ms (n = 5), indicating that YC-1 did not significantly alter the time course of activation.

In contrast to the activation process, YC-1 accelerated Kv current decay in a concentration-dependent fashion (Fig. 2A). Therefore, we fitted the data to a double exponential function and obtained two time constants. We assumed that the time constant of the faster component represented the development of a drug-induced blockade of the Kv current (τ_D), and that the slow time constant represented the slow and partial process of inactivation, which was due to intrinsic inactivation (9, 17). To determine the apparent association and dissociation rate constants (k_{+1} and k_{-1}, respectively), we plotted the data shown in Fig. 2 as the reciprocal of the time constant for Kv current inhibition at +40 mV vs. drug concentration (Fig. 3). Using this approach, we calculated a k_{+1} of 0.36 ± 0.01 $\mu M^{-1} \cdot s^{-1}$, and a k_{-1} of 3.44 ± 0.22 s^{-1}. On the basis of the first-order reaction between the drug and channel, the theoretically derived K_d value ($K_d = k_{-1} / k_{+1}$) was determined to be 9.56 ± 0.11 μM in the presence of YC-1. This result is in good agreement with the K_d value calculated by fitting the concentration–response curves (Fig. 2).

Effect of YC-1 on steady-state activation and inactivation of Kv channels

The voltage-dependence of activation and steady-state inactivation was evaluated to investigate whether YC-1–induced inhibition of the Kv current was due to a shift of the activation or inactivation curve. Activation curves were obtained using the tail current by a typical two-pulse protocol and the data were fit to a Boltzmann function. As shown in Fig. 4A, application of 10 μM YC-1 did not shift the steady-state activation curve. The half-maximal activation potential ($V_{1/2}$) and slope value (k) were −11.50 ± 0.42 mV and 8.66 ± 0.37, respectively, for the control conditions and −12.15 ± 0.83 mV and 9.62 ± 0.73, respectively, in the presence of 10 μM YC-1.

The steady-state inactivation kinetics of the Kv currents were also investigated in the absence and presence of 10 μM YC-1. The currents were obtained using a conventional double-pulse protocol (test step to +40 mV after an 8-s conditioning pre-pulse at different voltages). The inactivation data were fit to another Boltzmann function. As shown in Fig. 4B, 10 μM YC-1 did not change the voltage dependence of the inactivation kinetics of the Kv channels, suggesting that YC-1 does not interact strongly with the inactivated state of Kv channels. The potential of the half-inactivation ($V_{1/2}$) and slope value (k) were −34.67 ± 0.57 mV and 8.64 ± 0.47, respectively, for the control conditions and −36.16 ± 0.66 mV and 8.30 ± 0.31, respectively, in the presence of 10 μM

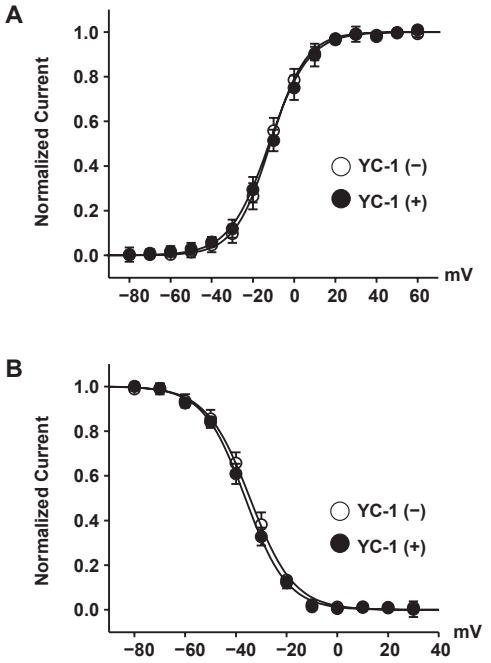

Fig. 4. Effect of YC-1 on the activation and steady-state inactivation properties of Kv channels. A: Activation curves in the absence (open circle) and presence (closed circle) of 10 μM YC-1 (n = 6). B: Steady-state inactivation curves in the absence (open circle) and presence (closed circle) of 10 μM YC-1 (n = 4). Data were fit to the Boltzmann equation (see Materials and Methods).

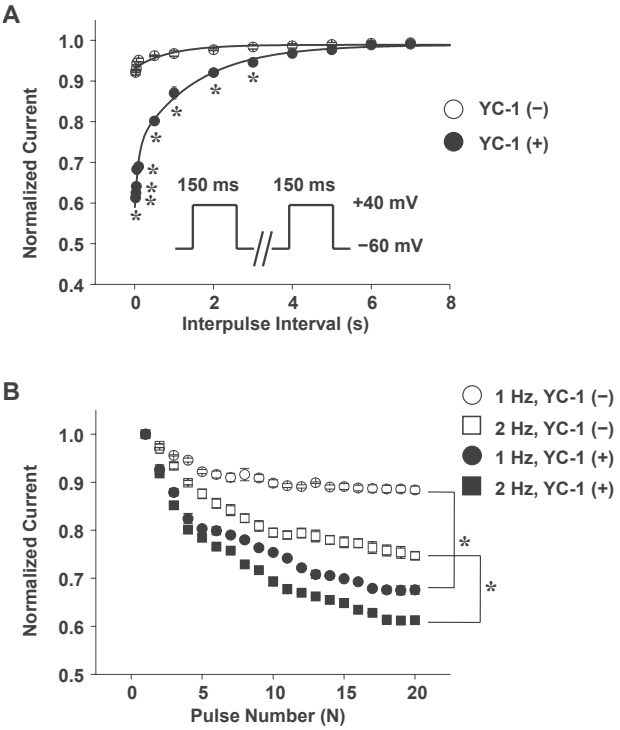

Fig. 5. Use-dependent effects of YC-1 on Kv channels. A: The time course of the recovery currents obtained from the second pulse followed by the first pulse in the absence and presence of YC-1 as described in the inset. The peak current elicited by the second test pulse was normalized by the currents evoked by the corresponding pre-pulses and plotted as a function of various time intervals from 20 ms to 7 s. The solid line represents the recovery kinetics of the Kv current under control conditions (open circle, n = 5) and in the presence of YC-1 (closed circle, n = 4). B: Frequency-dependent inhibition of the Kv current by YC-1. Twenty 150-ms depolarizing pulses of +40 mV were applied in rapid succession in the absence (open circle, open square) and presence of 10 μM YC-1 (closed circle, closed square) with a holding potential of −60 mV at frequencies of 1 and 2 Hz. The peak amplitude of current obtained at two different frequencies was normalized by the peak amplitude of the current at the first pulse, and plotted against the pulse number (n = 4). *$P < 0.05$, compared to the control.

YC-1.

Use-dependent inhibition of Kv currents by YC-1

Typical recovery kinetics of Kv currents in the absence and presence of 10 μM YC-1 are shown in Fig. 5. The recovery process was measured using a double-pulse protocol as shown in Fig. 5A (inset). The inter-pulse interval was varied from 20 ms to 7,000 ms. The data for recovery from inactivation in the absence or presence of 10 μM YC-1 were fit to single exponential functions with recovery time constants of 890.49 ± 105.64 ms under control conditions and 1,515.31 ± 169.36 ms in the presence of YC-1. The slower recovery time constant might explain the use-dependent blockade of the Kv current by YC-1. In agreement with this prediction, Fig. 5B also shows the use-dependence of the YC-1–block of the Kv current. Application of 20 repeated depolarizing pulses of +40 mV at 1 and 2 Hz progressively decreased the peak amplitude in the presence of 10 μM YC-1. Under control conditions, the peak amplitude of the Kv current measured at the final pulse showed a weak frequency dependence, decreasing by 11.62 ± 0.76% at a frequency of 1 Hz and by 25.34 ± 0.81% at a frequency of 2 Hz. In the presence of 10 μM YC-1, however, the peak amplitude showed a relatively strong frequency dependence, decreasing by 32.46 ± 0.90% at 1 Hz and by 38.77 ± 0.39% at 2 Hz. These data strongly suggest that the inhibitory effect of YC-1 is frequency (use)–dependent.

Effects of an alternative activator of sGC and of inhibitors of sGC and protein kinase G (PKG) on YC-1–induced inhibition of the Kv current

To confirm that YC-1–induced inhibition of the Kv current was not a result of sGC activation, we used an alternative sGC activator, Bay 41-2272, which is a pyrzolopyridine derivative (Fig. 6A, left) (18). Application of 1 μM Bay 41-2272 alone affected neither the Kv current nor the inhibitory effect of YC-1 on the Kv currents

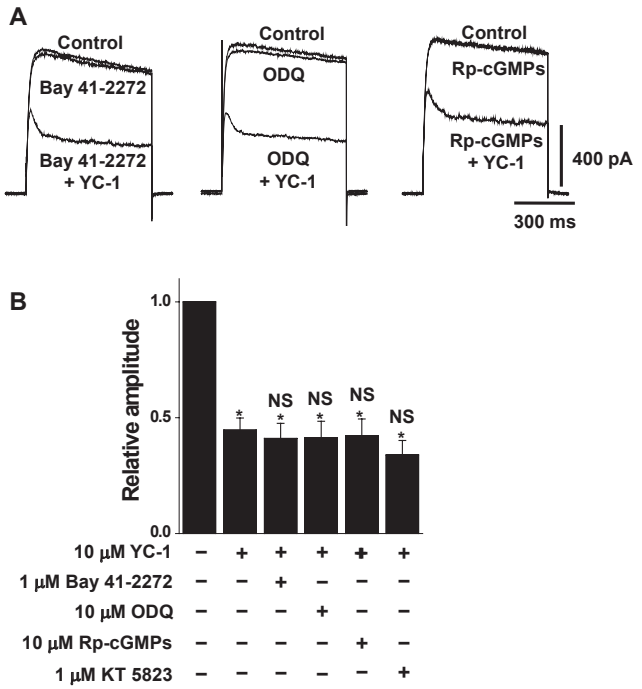

Fig. 6. Effect of an alternative sGC activator, an sGC inhibitor, and a PKG inhibitor on YC-1–induced inhibition of the Kv current. All current recordings were obtained by application of a depolarization pulse to +60 mV from a holding potential of −60 mV. Current traces obtained under control conditions, in the presence of Bay 41-2272, and with the additional application of 10 μM YC-1 (A, left, n = 4). Current traces obtained under control conditions, in the presence of ODQ, and with the additional application of 10 μM YC-1 (A, center, n = 6). Similar current traces obtained under control conditions, in the presence of Rp-cGMPs or KT 5823, and with the additional application of 10 μM YC-1 (A, right, n = 5). B: Summary of the results shown in panel A. *$P < 0.05$, compared to the control; NS = not significant compared to 10 μM YC-1 alone.

(10 μM YC-1 alone: 55.34 ± 5.21%, YC-1 + Bay 41-2247: 58.92 ± 6.48% inhibition, respectively, Fig. 6B). Furthermore, a specific inhibitor of sGC, ODQ (10 μM), had no effect on the Kv current, and ODQ together with YC-1 reduced the Kv current by 58.66 ± 7.28% (Fig. 6A, center), an amount not significantly different from that observed in the absence of ODQ (Fig. 6B). We also confirmed that cGMP – PKG signaling mechanisms were not involved in the YC-1–induced inhibition of Kv currents by pretreating the cells with a specific inhibitor of PKG, Rp-8-Br-PET-cGMPs (Rp-cGMPs) (Fig. 6A, right). Rp-cGMP failed to inhibit the Kv current and did not affect YC-1–induced inhibition of the Kv current. The application of KT 5823, another PKG inhibitor, yielded a similar result (YC-1 + Rp-cGMP: 57.82 ± 6.11% and YC-1 + KT 5823: 60.05 ± 6.23% inhibition, Fig. 6B). These results are strong evidence that YC-1 exerts its effect not via the sGC-PKG signaling pathway but by directly affecting Kv channels in coronary arterial smooth muscle cells.

Discussion

In this study, we investigated the effect of YC-1, a selective agonist of sGC and a blocker of hypoxia-inducible factor 1 (HIF-1) (19), on Kv channel function in smooth muscle cells from rabbit coronary arteries. Our results clearly suggest that YC-1 inhibits Kv channels in a state-, time, and use-dependent fashion independent of its sGC-activating properties and that it does not significantly alter the voltage-dependent activation and inactivation curves.

Several lines of evidence suggest that YC-1 inhibits Kv currents by acting directly on Kv channels, rather than by activating guanylyl cyclase: 1) Generally, activation of guanylyl cyclase increases cGMP levels and subsequently activates PKG, which hyperpolarizes smooth muscle by activating K^+ channels (20). However, we found that YC-1 reduced Kv-channel activity, suggesting that the inhibitory effect of YC-1 on Kv channel was not mediated by guanylyl cyclase; 2) the YC-1 concentration used here to inhibit the Kv current was lower than that needed for stimulation of guanylyl cyclase (4, 5); 3) Bay 41-2272, an sGC activator (18) that is structurally different from YC-1, had no effect on the Kv current; 4) pretreatment with sGC and PKG inhibitors do not alter Kv-channel activity or the inhibitory effect of YC-1; 5) the effect of YC-1 occurred rapidly, reaching steady-state inhibition within 2 min. This instantaneous effect of YC-1, and the short exposure time required to reach steady-state inhibition, cannot be explained simply by activation of guanylyl cyclase–related signal transduction mechanisms. Taken together, these results strongly suggest that YC-1 directly interacts with Kv channels to inhibit the Kv currents, independent of guanylyl cyclase.

Our results also suggest that YC-1 preferentially interacts with Kv channels that are in the open state. It accelerated the time course of the Kv current in a concentration-dependent fashion. Furthermore, it had little effect on the activation time course and had relatively little effect on the peak amplitude of the Kv current at the onset of depolarization. Finally, it did not shift the activation or steady-state inactivation curves, suggesting that it does not interact with Kv channels in their inactivated state but, instead, interacts with them in their open state.

Generally, four types of K^+ channels are present in vascular smooth muscle: ATP-sensitive K^+ (K_{ATP}), Ca^{2+}-activated K^+ (BK_{Ca}), inward rectifier K^+ (Kir), and voltage-dependent K^+ (Kv) channels (21). Among the K^+

channels, Kv channels plays a major role in determining the resting membrane potential and basal tone in some vascular smooth muscles (11, 12, 22). Furthermore, Kv channels are actively regulated by agonist-induced protein kinase–dependent signaling pathways. For example, vasoconstrictor-induced inhibition of K^+ channels is attributed to the activation of phospholipase C and the subsequent activation of protein kinase C (PKC) (23 – 26). Vasodilator-induced activation of K^+ channels is caused by activation of adenylyl cyclase and/or guanylyl cyclase and the consequent activation of protein kinase A (PKA) and/or PKG (9, 20, 27 – 30). Therefore, several drugs are indispensable for the study of Kv-channel modulation by various agonist-mediated signaling pathways. However, some undesired effects of these drugs complicate the accurate interpretation of experimental data. In fact, previous studies have suggested that some protein kinase inhibitors directly block Kv currents, independently of their kinase-inhibiting activity. For example, the PKC inhibitor bisindolylmaleimide (I) directly blocks stably expressed Kv1.5 channels in Chinese hamster ovary (CHO) cells (13) and Kv channels from freshly isolated coronary and mesenteric arterial smooth muscle cells (14, 31). Another PKC inhibitor, staurosporine, also blocks Kv1.3 channels stably expressed in CHO cells (32) and directly blocks the coronary Kv current (10). The PKA inhibitor H-89 blocks Kv channels in coronary smooth muscle cells (33) and Kv1.3 channels expressed in CHO cells (34), independently of PKA inhibition. Furthermore, Kv3.1 and Kv1.5 channels stably expressed in CHO cells are inhibited by the protein tyrosine kinase inhibitors genistein and AG-1478, respectively (35, 36). Here, we found convincing evidence that YC-1 directly inhibits Kv currents isolated from native coronary smooth muscle cells. These results might prove helpful in understanding the coronary vascular function related to cGMP-PKG signaling.

The Kv currents in vascular smooth muscle cells can be divided into the delayed rectifier current and transient current based on the different kinetics of activation and inactivation and the differences in pharmacological properties (9, 37). The delayed rectifier Kv currents show slow activation and inactivation kinetics in comparison to the transient Kv currents (38, 39). The Kv1.2, Kv1.5, and Kv2.1 α subunits were known to form the homotetrameric and heterotetrameric Kv channels with similar current kinetics to the native delayed rectifier Kv currents in vascular smooth muscle cells (40, 41). The molecular identity of the delayed rectifier Kv channels in vascular smooth muscle cells still, however, remains to be defined. Although we do not have direct evidence about the Kv-channel subtype that is inhibited by YC-1, our data imply that YC-1 may inhibit Kv1.2, Kv1.5, and/or Kv2.1 channel subunits in coronary arterial smooth muscle cells. Additional experiments need to be carried out to determine whether YC-1 inhibits Kv currents in HEK-293 cells transiently transfected with Kv1.2, Kv1.5, or Kv2.1 gene and whether inhibition of Kv1.5 (or Kv1.2 or Kv2.1) using siRNA can abolish the YC-1–mediated decrease in coronary arterial smooth muscle cells.

Several previous reports have suggested that the activation of the sGC-mediated increase in cGMP plays an important role in vasodilation by activation of BK_{Ca} channels (42, 43). Therefore, application of YC-1 could increase the K^+ efflux by activating BK_{Ca} channels, although this conflicts with the observation that YC-1 induces Kv-channel inhibition. However, in our experimental conditions, the activation of BK_{Ca} channels were minimized by the inclusion of 10 mM BAPTA, a Ca^{2+} chelator, in the pipette solution and the pretreatment with iberiotoxin (100 nM), a specific BK_{Ca}-channel inhibitor, in the bath solution. Also, it has been reported that agonist-mediated activation of BK_{Ca} channels through cAMP and cGMP-dependent protein kinases could be inhibited with treatment of 100 nM iberiotoxin (43). Therefore, we are confident that under our experimental conditions, there is a minimal contribution of BK_{Ca} to the Kv currents.

In conclusion, we have demonstrated that YC-1 directly inhibits the Kv current of rabbit coronary arterial smooth muscle cells in a state-, time-, and use-dependent fashion and that these inhibitory effects are completely independent of sGC activity and HIF-1. Since YC-1 is one of the most widely used agents in sGC-PKG signal transduction research, acts as an HIF-1 inhibitor, and has anticancer activity, caution is needed in the design and interpretation of functional studies of vascular physiology using YC-1.

Acknowledgments

This research was supported by Basic Science Research Program through the National Research Foundation of Korea (NRF) funded by the Ministry of Education, Science, and Technology (R0A-2007-000-20085-0, R13-2007-023-00000-0, and KRF-2008-313-E00046).

References

1 Wohlfart P, Malinski T, Ruetten H, Schindler U, Linz W, Schoenafinger K, et al. Release of nitric oxide from endothelial cells stimulated by YC-1, an activator of soluble guanylyl cyclase. Br J Pharmacol. 1999;128:1316–1322.

2 Russwurm M, Behrends S, Harteneck C, Koesling D. Functional properties of a naturally occurring isoform of soluble guanylyl cyclase. Biochem J. 1998;335:125–130.

3 González-Luis G, Cogolludo A, Moreno L, Lodi F, Tamargo J, Pérez-vizcaíno F, et al. Relaxant effects of the soluble guanylate cyclase activator and NO sensitizer YC-1 in piglet pulmonary

arteries. Biol Neonate. 2006;90:66–72.
4 Ko FN, Wu CC, Kuo SC, Lee FY, Teng CM. YC-1, a novel activator of platelet guanylate cyclase. Blood. 1994;84:4226–4233.
5 Mülsch A, Bauersachs J, Schäfer A, Stasch JP, Kast R, Busse R. Effect of YC-1, an NO-independent, superoxide-sensitive stimulator of soluble guanylyl cyclase, on smooth muscle responsiveness to nitrovasodilators. Br J Pharmacol. 1997;120:681–689.
6 Koesling D, Friebe A. Soluble guanylyl cyclase: structure and regulation. Rev Physiol Biochem Pharmacol. 1999;135:41–65.
7 Galle J, Zabel U, Hubner U, Hatzelmann A, Wagner B, Wanner C, et al. Effects of the soluble guanylyl cyclase activator, YC-1, on vascular tone, cyclic GMP levels and phosphodiesterase activity. Br J Pharmacol. 1999;127:195–203.
8 Seitz S, Wegner JW, Rupp, J, Watanabe M, Jost A, Gerhard R, et al. Involvement of K^+ channels in the relaxant effects of YC-1 in vascular smooth muscle. Eur J Pharmacol. 1999;382:11–18.
9 Nelson MT, Quayle JM. Physiological roles and properties of potassium channels in arterial smooth muscle. Am J Physiol. 1995;268:C799–C822.
10 Park WS, Son YK, Han J, Kim NR, Ko JH, Bae YM, et al. Staurosporine inhibits voltage-dependent K^+ current through a PKC-independent mechanism in isolated coronary arterial smooth muscle cells. J Cardiovasc Pharmacol. 2005b;45:260–269.
11 Shimoda LA, Sylvester JT, Sham JS. Inhibition of voltage-dependent K^+ current in rat intrapulmonary arterial myocytes by endothelin-1. Am J Physiol. 1998;274:L842–L853.
12 Bae YM, Kim A, Kim J, Park SW, Kim TK, Lee YR, et al. Serotonin depolarizes the membrane potential in rat mesenteric artery myocytes by decreasing voltage-gated K^+ currents. Biochem Biophys Res Commun. 2006;347:468–476.
13 Choi BH, Choi JS, Jeong SW, Hahn SJ, Yoon SH, Jo YH, et al. Direct block by bisindolylmaleimide of rat Kv1.5 expressed in Chinese hamster ovary cells. J Pharmacol Exp Ther. 2000;293:634–640.
14 Park WS, Son YK, Ko EA, Ko JH, Lee HA, Park KS, et al. The protein kinase C inhibitor, bisindolylmaleimide (I), inhibits voltage-dependent K^+ channels in coronary arterial smooth muscle cells. Life Sci. 2005;77:512–527.
15 Snyders DJ, Yeola SW. Determinants of antiarrhythmic drug action. Electrostatic and hydrophobic components of block of the human cardiac hKv1.5 channel. Circ Res. 1995;77:575–583.
16 Snyders DJ, Tamkun MM, Bennett PB. A rapidly activating and slowly inactivating potassium channel cloned from human heart. J Gen Physiol. 1993;101:513–543.
17 Roberds SL, Knoth KM, Po S, Blair TA, Bennett PB, Hartshorne RP, et al. Molecular biology of the voltage-gated potassium channels of the cardiovascular system. J Cardiovasc Electrophysiol. 1993;4:68–80.
18 Liu YC, Wu SN. Bay 41-2272, a potent activator of soluble guanylyl cyclase, stimulates calcium elevation and calcium-activated potassium current in pituitary GH_3 cells. Clin Exp Pharmacol Physiol. 2005;32:1078–1087.
19 Yeo EJ, Chun YS, Cho YS, Kim J, Lee JC, Kim MS, et al. YC-1: a potential anticancer drug targeting hypoxia-inducible factor 1. J Natl Cancer Inst. 2003;95:516–525.
20 Standen NB, Quayle JM. K^+ channel modulation in arterial smooth muscle. Acta Physiol Scand. 1998;164:549–557.
21 Ko EA, Han J, Jung ID, Park WS. Physiological roles of K^+ channels in vascular smooth muscle cells. J Smooth Muscle Res. 2008;44:65–81.
22 Smirnov SV, Aaronson PI. Ca^{2+}-activated and voltage-gated K^+ currents in smooth muscle cells isolated from human mesenteric arteries. J Physiol. 1992;457:431–454.
23 Hayabuchi Y, Davies NW, Standen NB. Angiotensin II inhibits rat arterial K_{ATP} channels by inhibiting steady-state protein kinase A activity and activating protein kinase Cε. J Physiol. 2001;530:193–205.
24 Park WS, Ko EA, Han J, Kim NR, Earm YE. Endothelin-1 acts via protein kinase C to block K_{ATP} channels in rabbit coronary and pulmonary arterial smooth muscle cells. J Cardiovasc Pharmacol. 2005;45:99–108.
25 Ledoux J, Warner ME, Brayden JE, Nelson MT. Calcium-activated potassium channels and the regulation of vascular tone. Physiology. 2006;21:69–78.
26 Park WS, Kim NR, Youm JB, Warda M, Ko JH, Kim SJ, et al. Angiotensin II inhibits inward rectifier K^+ channels in rabbit coronary arterial smooth muscle cells through protein kinase Cα. Biochem Biophys Res Commun. 2006;341:728–735.
27 Robertson BE, Schubert R, Hescheler J, Nelson MT. cGMP-dependent protein kinase activates Ca^{2+}-activated K^+ channels in cerebral artery smooth muscle cells. Am J Physiol. 1993;265:C299–C303.
28 Aiello EA, Walsh MP, Cole WC. Phosphorylation by protein kinase A enhances delayed rectifier K^+ current in rabbit vascular smooth muscle cells. Am J Physiol. 1995;268:H926–H934.
29 Wellman GC, Quayle JM, Standen NB. Calcitonin gene-related peptide (CGRP) activates an ATP-sensitive potassium (K_{ATP}) current in pig coronary vascular smooth muscle cells via a cyclic AMP-dependent protein kinase (PKA). J Physiol. 1998;507:117–129.
30 Son YK, Park WS, Ko JH, Han J, Kim NR, Earm YE. Protein kinase A-dependent activation of inward rectifier potassium channels by adenosine in rabbit coronary smooth muscle cells. Biochem Biophys Res Commun. 2005;337:1145–1152.
31 Kim A, Bae YM, Kim J, Kim B, Ho WK, Earm YE, et al. Direct block by bisindolylmaleimide of the voltage-dependent K^+ currents of rat mesenteric arterial smooth muscle. Eur J Pharmacol. 2004;483:117–126.
32 Choi JS, Hahn SJ, Rhie DJ, Jo YH, Kim MS. Staurosporine directly blocks $K_V1.3$ channels expressed in Chinese hamster ovary cells. Naunyn Schmiedebergs Arch Pharmacol. 1999;359:256–261.
33 Son YK, Park WS, Kim SJ, Earm YE, Kim N, Youm JB, et al. Direct inhibition of a PKA inhibitor, H-89 on K_V channels in rabbit coronary arterial smooth muscle cells. Biochem Biophys Res Commun. 2006;341:931–937.
34 Choi JS, Choi BH, Hahn SJ, Yoon SH, Min DS, Jo Y, et al. Inhibition of Kv1.3 channels by H-89 (N--[2-(p-bromocinnamylamino) ethyl]-5-isoquinolinesulfonamide) independent of protein kinase A. Biochem Pharmacol. 2001;61:1029–1032.
35 Choi BH, Choi JS, Rhie DJ, Yoon SH, Min DS, Jo YH, et al. Direct inhibition of the cloned Kv1.5 channel by AG-1478, a tyrosine kinase inhibitor. Am J Physiol. 2002;282:C1461–C1468.
36 Choi BH, Park JH, Hahn SJ. Open channel block of Kv3.1 currents by genistein, a tyrosine kinase inhibitor. Korean J Physiol Pharmacol. 2006;10:71–77.
37 Iida H, Jo T, Iwasawa K, Morita T, Hikiji H, Takato T, et al. Molecular and pharmacological characteristics of transient voltage-dependent K^+ currents in cultured human pulmonary arterial smooth muscle cells. Br J Pharmacol. 2005;146:49–59.

38 Beech DJ, Bolton TB. Two components of potassium current activated by depolarization of single smooth muscle cells from the rabbit portal vein. J Physiol. 1989;418:293–309.
39 Halliday FC, Aaronson PI, Evans AM, Gurney AM. The pharmacological properties of K^+ currents from rabbit isolated aortic smooth muscle cells. Br J Pharmacol. 1995;116:3139–3148.
40 Kerr PM, Clément-Chomienne O, Thorneloe KS, Chen TT, Ishii K, Sontag DP, et al. Heteromultimeric Kv1.2-Kv1.5 channels underlie 4-aminopyridine-sensitive delayed rectifier K^+ current of rabbit vascular myocytes. Circ Res. 2001;89:1038–1044.
41 Lu Y, Hanna ST, Tang G, Wang R. Contributions of Kv1.2, Kv1.5 and Kv2.1 subunits to the native delayed rectifier K^+ current in rat mesenteric artery smooth muscle cells. Life Sci. 2002;71:1465–1473.
42 Carrier GO, Fuchs LC, Winecoff AP, Giulumian AD, White RE. Nitrovasodilators relax mesenteric microvessels by cGMP-induced stimulation of Ca-activated K channels. Am J Physiol. 1997;273:H76–H84.
43 Wu BN, Chen CF, Hong YR, Howng SL, Lin YL, Chen IJ. Activation of BK_{Ca} channels via cyclic AMP- and cyclic-dependent protein kinases by eugenosedin-A in rat basilar artery myocytes. Br J Pharmacol. 2007;152:374–385.